Journal of Biomechanics 40 (2007) 1145–1152

JOURNAL OF BIOMECHANICS

www.elsevier.com/locate/jbiomech
www.JBiomech.com

The influence of deceleration forces on ACL strain during single-leg landing: A simulation study

Choongsoo S. Shin[a,*], Ajit M. Chaudhari[a], Thomas P. Andriacchi[a,b,c]

[a]Department of Mechanical Engineering, Division of Biomechanical Engineering, Stanford University, 496 Lomita Mall, Durand Building Room 224, Stanford, CA 94305-4038, USA
[b]Department of Orthopedics, Stanford University, Stanford, CA, USA
[c]Bone and Joint Center, Palo Alto VA, Palo Alto, CA, USA

Accepted 4 May 2006

Abstract

Anterior cruciate ligament (ACL) injury commonly occurs during single limb landing or stopping from a run, yet the conditions that influence ACL strain are not well understood. The purpose of this study was to develop, test and apply a 3D specimen-specific dynamic simulation model of the knee designed to evaluate the influence of deceleration forces during running to a stop (single-leg landing) on ACL strain. This work tested the conceptual development of the model by simulating a physical experiment that provided direct measurements of ACL strain during vertical impact loading (peak value 1294 N) with the leg near full extension. The properties of the soft tissue structures were estimated by simulating previous experiments described in the literature. A key element of the model was obtaining precise anatomy from segmented MR images of the soft tissue structures and articular geometry for the tibiofemoral and patellofemoral joints of the knee used in the cadaver experiment. The model predictions were correlated (Pearson correlation coefficient 0.889) to the temporal and amplitude characteristic of the experimental strains. The simulation model was then used to test the balance between ACL strain produced by quadriceps contraction and the reductions in ACL strain associated with the posterior braking force. When posterior forces that replicated in vivo conditions were applied, the peak ACL strain was reduced. These results suggest that the typical deceleration force that occurs during running to a single limb landing can substantially reduce the strain in the ACL relative to conditions associated with an isolated single limb landing from a vertical jump.

Keywords: Anterior cruciate ligament strain; ACL injury; Knee model; Single-leg landing; Deceleration force

1. Introduction

Anterior cruciate ligament (ACL) injury is very common during sport activities and frequently occurs in the absence of contact with another player or object (Boden et al., 2000; Griffin et al., 2000). While it is reported that noncontact ACL injuries often occur during landing or deceleration prior to a change of direction (Boden et al., 2000), the mechanism of ACL injury is not well understood. Anterior forces on the tibia, internal/external rotational torque, and valgus torque contribute to strain in the ACL in controlled in vitro and in vivo studies with low-magnitude quasi-static loads (Markolf et al., 1995; Woo et al., 1999; Fleming et al., 2001). However, a recent study of individuals performing a single-leg run-to-stop revealed that anterior translation of the tibia may not occur during this activity (Chaudhari et al., 2004). Instead, posterior forces on the tibia were observed during the first 100 ms after foot strike, due to the deceleration forces acting at the foot. These forces caused posterior tibial translation in most subjects, which would seem to protect the ACL from injury. However, the effect of this observed combination of loads on ACL strain remains unknown.

*Corresponding author. Tel.: +1 650 736 0807; fax: +1 650 725 1587.
E-mail address: scslove@stanford.edu (C.S. Shin).

0021-9290/$ - see front matter
doi:10.1016/j.jbiomech.2006.05.004

To understand the mechanism of ACL injuries, estimating the strain of the ACL is essential. ACL strain has mainly been measured using in vivo measurement with implanted displacement transducers (Beynnon et al., 1992; Fleming et al., 2001) or in vitro measurement using various techniques (Markolf et al., 1995; Woo et al., 2006). Computer simulations have also predicated ligament forces (Pandy and Shelburne, 1997; Song et al., 2004).

Simulation studies have provided considerable insight into the biomechanics of the knee joint (Crowninshield et al., 1976; Andriacchi et al., 1983; Garg et al., 1990; Blankevoort et al., 1991; Shelburne and Pandy, 1997; Yu et al., 2001; Chen et al., 2001; Caruntu and Hefzy, 2004). However, most of these models use generic anatomical geometry and are designed only to predict static or quasi-static characteristics of the knee joint such as passive flexion and rotational stiffness. Predictions of ACL strain during dynamic landing motions have not been performed using a model validated for the estimation of ACL strain. Thus there is a need for a knee model that predicts ACL strain under dynamic loading conditions that occur in vivo during sports activities similar to those that result in ACL injuries.

The purpose of this study was to develop, test, and apply a 3D specimen-specific dynamic simulation model of the knee designed to test the influence of deceleration forces on ACL strain during run-to-stop single-leg landing.

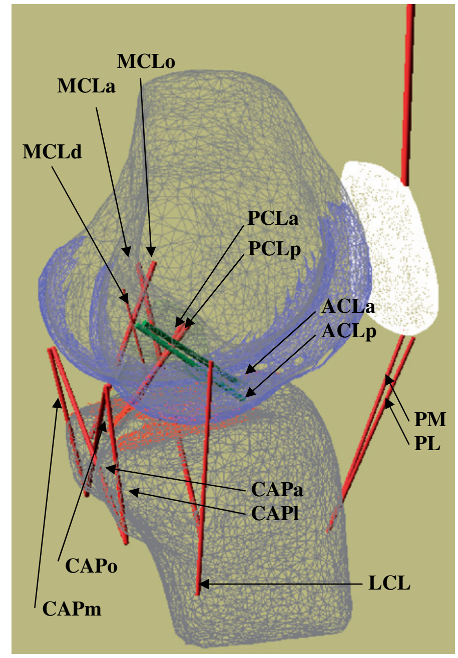

Fig. 1. Schematic of the knee model showing 14 ligament bundles. ACL bundles are shown green. The anterior and posterior bundle of ACL (ACLa and ACLp); the anterior and posterior bundle of PCL (PCLa and PCLp); the LCL; anterior, oblique, and deep bundle of MCL (MCLa, MCLo, and MCLd); the medial, lateral, oblique popliteal, and arcuate politeal bundle of posterior capsules (CAPm, CAPl, CAPo, and CAPa); and the medial and lateral patellar ligament (PM and PL).

2. Methods

A 3D dynamic specimen-specific knee model (Fig. 1) and the simulated experimental apparatus were created to investigate the influence of various loading configurations on ACL strain during landing motions. The knee model was constructed from the MRI of a cadaver specimen that was used in an experimental study (Fig. 2a and b) to replicate vertical impact loading during single limb landing (Withrow et al., 2006). Soft tissues were modeled as nonlinear elastic elements with properties obtained from the literature. The experimental apparatus (Fig. 2b) was simulated with similar dimensions, mass, and the same musculotendinous properties as the physical experimental apparatus (Fig. 2a). A specimen-specific validation of ACL strains was performed by comparing predicted ACL strains to experimental measurements under identical loading and limb alignment. No parameters in the knee model were adjusted for the validation test; finally, physiological levels of external posterior force were applied to investigate the effect of deceleration force on ACL strain.

Model anatomy was obtained from MRI (3D-SPGR sequence, FOV $140 \times 140\,\mathrm{mm}^2$, matrix 256×256, slice

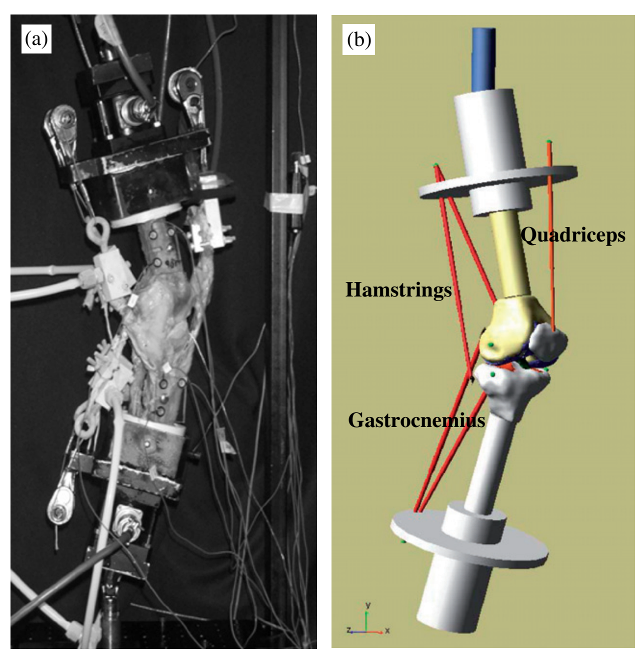

Fig. 2. (a) The experimental apparatus used for validation (photo by courtesy of Dr. Withrow). (b) The simulated dynamic single-leg landing apparatus with the specimen-specific knee model showing five musculotendinous bundles.

thickness 1.5 mm). The distal femur, the proximal tibia, the patella, and articular cartilage of the cadaveric knee were segmented using custom software (Koo et al., 2005) and imported into a dynamic simulation package (ADAMS 2003, MSC.Software, Inc., Santa Ana, CA). Femoral and tibial reference frames were placed at the midpoint of the femoral trans-epicondylar axis and at the midpoint of the tibial plateau, respectively, and the six-degrees-of-freedom kinematic motion of the knee was described using a standard technique (Andriacchi et al., 1998). The knee used in this model was representative of an average sized male by bicondylar width (89 mm vs. a range of 87.5–93.5 mm, Shelbourne et al., 1998) and inspected for indications of surgery, malalignment, or radiographic deformities before cadaver test. The height-of-patella ratio (Blackburne-Peel index = 0.94; Insall–Salvati index = 1.1) also suggests normal patellofemoral movement (Blackburne and Peel, 1977; Insall and Salvati, 1971).

Ligaments and capsules were modeled as nonlinear elastic line elements. The ACL and the posterior cruciate ligament (PCL) were modeled using two bundles, as done in previous simulation models (Yu et al., 2001; Blankevoort et al., 1991; Abdel-Rahman and Hefzy, 1998), since two functional bundles have been identified in clinical and cadaver studies (Girgis et al., 1975; Woo et al., 2002). The composition of the other ligaments was based on previous knee models (Yu et al., 2001; Abdel-Rahman and Hefzy, 1998) (Table 1). The lateral collateral ligament (LCL) was modeled as a single element, while the medial collateral ligament (MCL) was modeled as three elements, including the anterior, the oblique, and the deep fiber. The posterior capsule was represented by four fibers: the medial, the lateral, the oblique popliteal, and the arcuate popliteal fiber. The locations of the origins and the insertions of the ACL and PCL were segmented from sagittal MRI and transferred with other bone geometries. Two functional bundle insertion regions for each cruciate ligament into femur and tibia were identified in reconstructed geometries as previously quantified (Harner et al., 1999). The centroids of each region were estimated to be the insertion points of each bundle. The locations of MCL, LCL, and posterior capsule were determined differently, because segmentation of these structures to determine the locations for multiple bundles was inappropriate due to broad attachments and poor view from sagittal MRI with the chosen resolution. The bundles of the MCL, LCL, and posterior capsule (Fig. 1) were placed over the appropriate bony landmarks (Clarke et al., 2001; Garg and Walker, 1990; Reicher, 1993) using the same method and bundle orientation as described by Yu et al. (2001).

The stiffness of each ligament or capsule fiber was formulated by combining two linear springs as follows (Table 2):

$$F = \begin{cases} 0, & \varepsilon \leqslant 0, \\ \frac{k}{2}(L - L_0), & 0 \leqslant \varepsilon \leqslant 2\varepsilon_1, \\ k[L - (1+\varepsilon_1)L_0], & 2\varepsilon_1 \leqslant \varepsilon, \end{cases} \qquad (1-3)$$

where L is the current length of the ligament; L_0 is the slack length; ε is the engineering strain ($\varepsilon = (L-L_0)/L_0$); ε_1 is specified as 0.03; and k is the stiffness coefficient of the ligament obtained from previous studies (Yu et al., 2001; Abdel-Rahman and Hefzy, 1998; Woo et al., 1991; Noyes et al., 1984; Cooper et al., 1993). Eq. (3) represents the terminal stiffness, similar to other studies (Yu et al., 2001; Abdel-Rahman and Hefzy, 1998), while Eq. (2) represents the toe region. Reference strains were assigned to the ligaments based on previous knee models (Shelburne and Pandy, 1997; Blankevoort et al., 1991) (Table 2).

The contact forces at the tibiofemoral and patellofemoral articulations were defined using the penalty

Table 1
Composition of ligamentous bundles and musculotendinous bundles

Structure	Number of bundles
Anterior cruciate ligament	2
Posterior cruciate ligament	2
Lateral collateral ligament	1
Medial collateral ligament	3
Posterior capsule	4
Patellar ligament	2
Quadriceps	1
Hamstraings	2
Gastrocnemius	2

Table 2
Properties of ligaments

Ligament	Stiffness (N/mm)	Reference strain	Slack length (mm)
ACLa	108.0	0.02	35.21
ACLp	108.0	0.02	34.61
PCLa	125.0	−0.10	34.78
PCLp	60.0	−0.02	26.34
LCL	91.3	0.02	68.78
MCLa	27.9	0.02	45.51
MCLo	21.1	0.02	35.16
MCLd	72.2	0.02	58.19
CAPm	52.6	0.02	38.20
CAPl	54.6	0.02	39.85
CAPo	21.4	0.02	63.18
CAPa	20.8	0.02	62.15
PM	300.0	-0.05	56.78
PL	300.0	-0.05	56.78

Stiffness data adapted from Yu et al. (2001), Abdel-Rahman and Hefzy (1998), Woo et al. (1991), Noyes et al. (1984), Cooper et al. (1993). Reference strains adapted from Shelburne and Pandy (1997), Blankevoort et al. (1991). The slack lengths of ligaments were calculated using the measured data from reconstructed MR images and assigned reference strain at full extension.

regularization of normal contact force constraints (Lötstedt, 1982), whose algorithm is implemented in the ADAMS solver. The nonlinear stiffness parameters used with this algorithm were based on measured properties for articular surface contact (Nam et al., 2004; Oni and Morrison, 1998), and they ensured that the maximum penetration depth never exceeded the cartilage thickness. While not explicitly estimating the deformation patterns of the entire articulating surfaces, this method allowed the resultant elastic characteristic of cartilage to be included. Friction at the articular contact was assumed to be negligible since the surfaces represent healthy articular cartilage (Mow et al., 1993).

The patellar ligament was modeled by two bundles (medial and lateral) and placed based on the origin (most distal point on patella) and insertion (tibial tuberosity) as viewed in the MRI. The stiffness of the patellar ligament was obtained from previous studies (Noyes et al., 1984; Cooper et al., 1993). In addition, three musculotendinous groups including the quadriceps, the hamstrings (biceps femoris and semitendinosus), and the gastrocnemius (medial and lateral heads), were modeled to represent the in vivo dynamic resistance to simulated landing motions. The insertions of the quadriceps tendon, biceps femoris, and semitendinosus and origins of the medial and lateral gastrocnemius were identified in MRI and segmented to determine their insertion locations in the model, while the opposite attachments of those muscle units to the apparatus were chosen to match the dimensions of the physical apparatus (Fig. 2a and b). In the physical experimental apparatus (Withrow et al., 2006), musculotendinous units were reproduced using aircraft cables with appropriate stiffness (Fig. 2a). These cables and their mounting points were replicated in the simulation model with the same stiffness and pretension (Fig. 2b). In both the cadaver apparatus and simulation model, the tensions in these musculotendinous units were chosen to hold the initial knee flexion angle at 25° before external loading was applied. This initial flexion angle was selected in the physical experimental apparatus (Withrow et al., 2006) because the average knee flexion angle at foot strike was reported as 23° for landing from a jump motion (Colby et al., 2000). This initial angle chosen for the experiment was replicated in the simulation model. The compositions of the ligaments, capsules, and musculotendinous elements are summarized in Table 1.

In both the physical experiment apparatus and the simulation model, the proximal end of the femur and distal end of the tibia were rigidly potted in containers which were connected to spherical joints, allowing free rotation but no translation. The spherical joint at the proximal end was connected to the mounting apparatus through a linear slide, allowing vertical motion (Fig. 3). The model predicted ACL strain with unconstrained tibiofemoral motion (six-degree-of-freedom model) based on previous studies (Woo et al., 1999).

The knee model and the simulated experimental apparatus were tested for this specific specimen by comparing the results of the physical impact force experiment to those of the simulation. In the physical experimental apparatus, the impact force was applied at the top of the femur by free dropping of a weight (Fig. 3); the impact force profile was collected using a load cell; the deformation of the ACL was measured using a differential variable reluctance transducer on the ACL (Withrow et al., 2006). The impact force profile collected from the experiment was imported as the input to drive the simulation model under the same initial flexion angle obtained by the same muscle pretensions. The results of the physical test and simulation were compared for knee flexion angle, the quadriceps force, and relative ACL strain. Relative ACL strain (elongation of ACL relative to pre-impact length, Fleming et al., 1994) was used for the validation because relative ACL strain was the only quantity measured in the experiment, and this method allows the impact to be the sole cause for increase in strain (Withrow et al., 2006). In this process, no parameters of the simulation model were adjusted to calibrate the responses. The results were merely compared for validation purposes. The

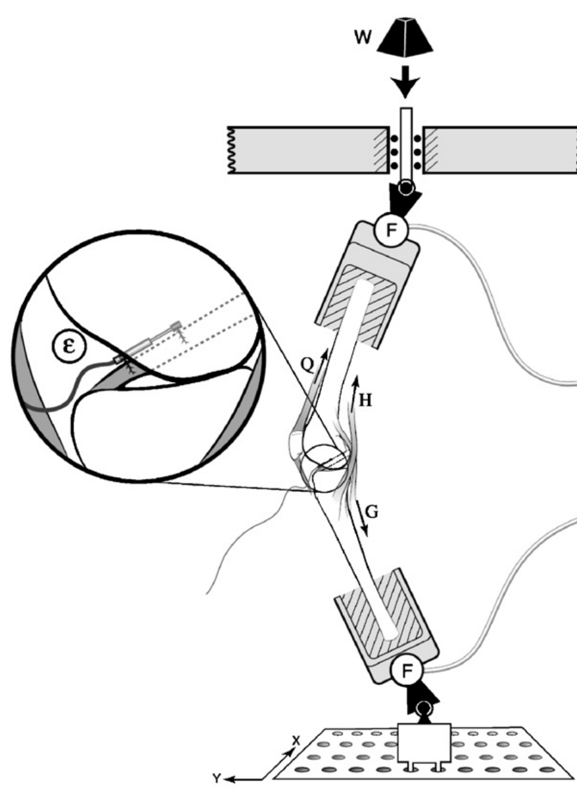

Fig. 3. Schematic of the single-leg landing experimental device (Withrow et al., 2006, copyright 2006 by the American orthopedic Society for Sports Medicine, Reprinted by permission of Sage Publications Inc.).

similarities of responses from experiment and simulation were quantitatively measured using Pearson correlation coefficients between the experimental results and the simulation results from −0.01 to 0.08 s.

After the specimen-specific validation test, a parametric study was performed to investigate the influence of increasing the external posterior force on ACL strain during single-leg landing using the same initial flexion (25°) and musculotendinous pretensions as the validation test. In addition to the same dynamic impact load, an external posterior force was applied at the midpoint of the trans-tibial line at four different magnitudes. The dynamic profile and magnitudes of external posterior force were based on a previous in vivo study of a run-to-stop single-leg landing maneuver (Chaudhari et al., 2004) where the ratio of posterior force to vertical impact force reached a peak of 0.30. Therefore, external posterior force was applied with a range of values from 0% to 30% of the vertical impact force in increments of 10%, and the response of the average strain in the two bundles of the ACL to this increasing posterior force was examined.

3. Results

The vertical impact forces in the experiment and the simulation both reached a peak of 1294 N within 2 ms (Fig. 4). The quadriceps force in the simulation showed a similar pattern to the experiment (Fig. 5). The peak quadriceps force in the simulation was 1189 N, which was 7.8% less than the peak force observed in the experiment, 1290 N. The quadriceps force in the experiment (simulation) increased at a rate of 40 N/ms (47 N/ms) and reached the peak in 27 ms (22 ms). The Pearson correlation coefficient between temporal data of quadriceps force from experiment and simulation was 0.943.

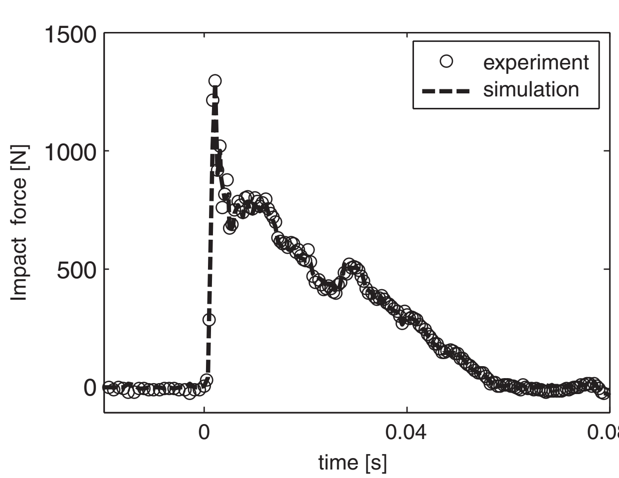

Fig. 4. The temporal profile of the impact force (N) applied in the experiment and the simulation (validation test).

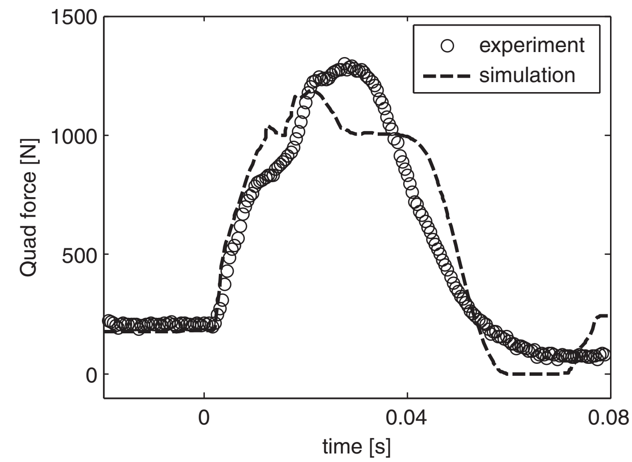

Fig. 5. Quadriceps force (N) measured from experiment and simulation (validation test).

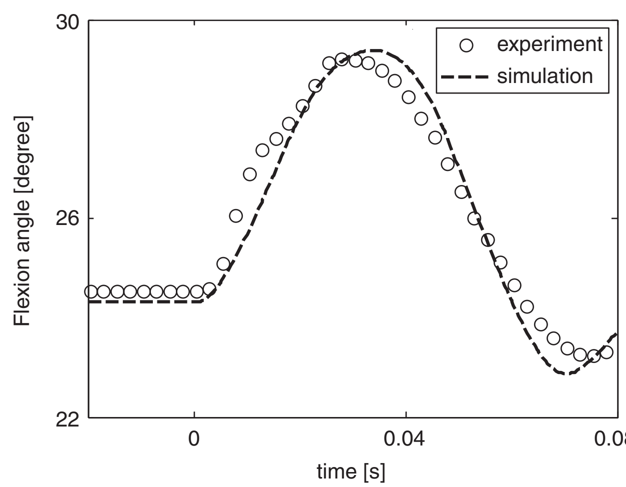

Fig. 6. Flexion angle (°) measured from experiment and simulation (validation test).

The initial knee flexion angle was about 25° before applying the impact force in both experiment (24.5°) and simulation (24.3°), but the flexion angle increased up to 29.5° in 30 ms as a result of the impact force input (Fig. 6). The flexion angles in the experiment and the simulation increased by 4.7° and 5.1°, respectively (a difference of 7.9%; Pearson correlation coefficient = 0.983).

The strains of the anteromedial and posterolateral bundles in the simulation were averaged to compare the experimental results (Fig. 7). The peak relative strain in the ACL was 2.5% in the experiment and 2.1% in the simulation (Pearson correlation coefficient = 0.889), and the strains reached peak values within 25 ms of each other.

Over the entire range of applied posterior forces, the ACL strain reached its peak value within the first 40 ms

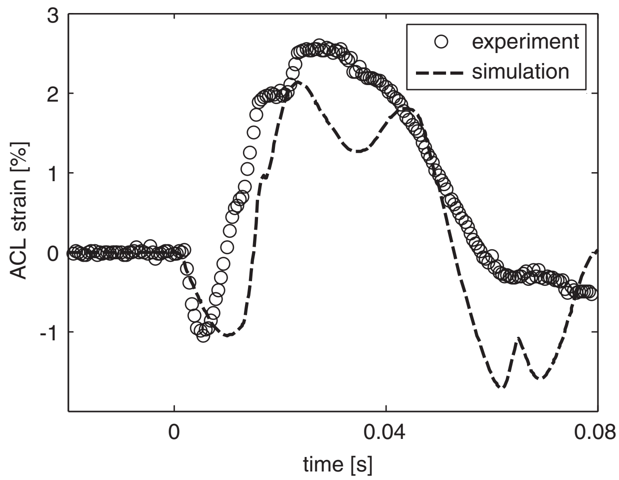

Fig. 7. Relative ACL strain (%) measured from experiment and average relative ACL strain from simulation (validation test). ACL strain reached its peak value within 40 ms after initial impact.

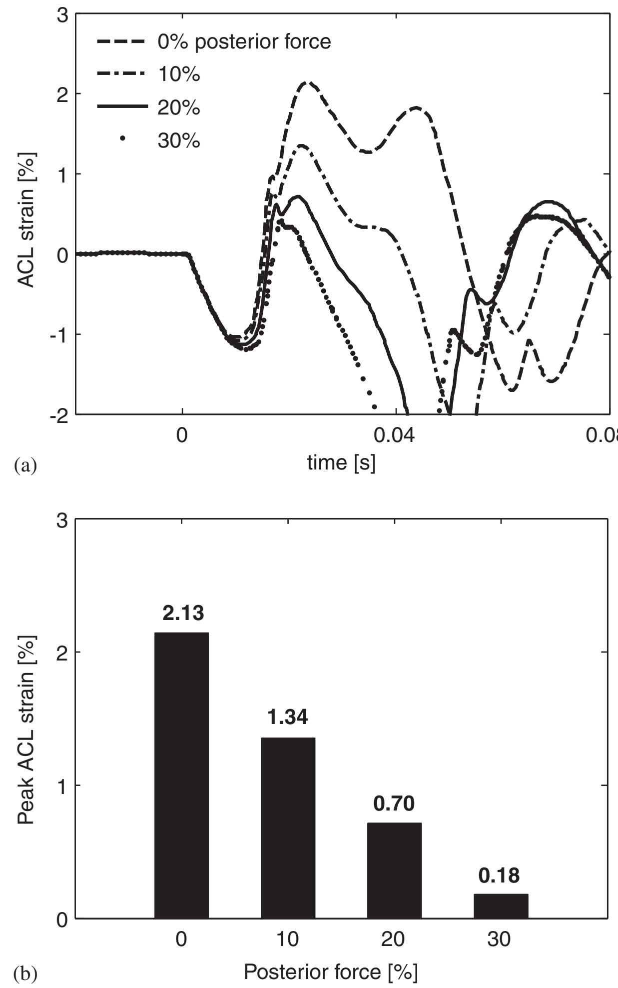

Fig. 8. (a) Temporal behavior of average relative ACL strain (%) with an increment of posterior forces (% of impact force, N) from four parametric simulations. (b) Peak values of the ACL strain curves shown in (a), showing a 91% decrease when the posterior force was increased from 0% to 30% magnitude of the impact force.

after initial impact (Fig. 8a). As the posterior force was increased from 0% to 30% of the vertical impact force, the peak average relative strain in the ACL was reduced from 2.13% to 0.18% (Fig. 8b). The external posterior force corresponding to 30% of the vertical impact force in the landing simulation demonstrated that the peak relative strain in the ACL was reduced by a factor of 10 compared with the strain without posterior force.

4. Discussion and conclusion

This study demonstrated that the posterior deceleration force during a run-to-stop can protect the ACL by reducing the peak strain produced by quadriceps contraction. The external posterior force was caused by decelerating the body's forward momentum. The findings of this study suggest that excessive quadriceps force is an unlikely mechanism of ACL injury when an external posterior force is present, because for the quadriceps to cause an injury through anterior translation it first would have to overcome the sizable posterior forces. Thus, other mechanisms such as valgus rotation, internal rotation, or a combination of the two, which are not protected by external loading, may be more relevant to ACL injuries (Hewett et al., 2005; Olsen et al., 2004; McLean et al., 2004). In real activities such as a run-to-stop or a vertical landing, the total combined loading applied to the knee may include other forces or moments as well, such as externally applied valgus or tibial internal rotation moments. One main difference between run-to-stop and simple drop landing is the posterior force due to horizontal deceleration during a run-to-stop. Therefore, the results of this study should be considered in light of the fact that the complete complexity of loading during single limb landing was not simulated.

The purpose of this study was to use a model simulation to isolate the influence of the posterior force on ACL strain since in many sports injuries occur during run-to-stop activities rather than in drop landings from a height. A number of assumptions were used to construct the model used in this study. The quadriceps, hamstrings, and gastrocnemius were assumed to be passively tensioned before the impact to simulate eccentric contraction in the quadriceps. The assumption was based on previous reports that peak tension in the ligament occurred within 40 ms of the initial impact (Fig. 8a), which is shorter than the time needed for an active response (Burke et al., 1991). In addition, quadriceps activity has been shown to increase slowly before landing, and during high deceleration or landing the quadriceps undergoes eccentric contraction (Colby et al., 2000). These studies support the assumption of constant activation with pretensioned muscles in this model. In such a situation, passive stretch of muscle fibers should account for most of the force generated. Other assumptions for the model included ligament material properties obtained from the literature rather than the specific material properties of the cadaver specimen, and an assumption that the contribution of the meniscus was negligible for the purposes of this study. Another assumption that should be considered carefully is that the model does not account for wrapping of the ACL around the intercondylar notch of the femur or the interaction between the bundles. However, since this study was conducted with the knee near 25° of flexion with no external rotation, no interference between the ACL and intercondylar notch is likely (Fung and Zhang, 2003; Withrow et al., 2006). Therefore, this assumption is unlikely to have affected the results of the study. Finally, the model was created using the anatomy of one average size knee specimen. Unlike previous simulation studies where a single generic model is generated from averaged anatomical data that may not represent any real specimen and whose results cannot be directly validated, this model represents a real individual of average size, and it has the distinct advantage of being directly validated against experimental results. While this approach permitted direct validation against experimental results, one must take care in generalizing these results to all knees. Even though some subtle differences may occur in anatomy and motions between individuals, the general trend of the influence of posterior force on ACL strain in this study should be preserved.

In consideration of the assumptions noted above, the predicted and measured ACL strain matched quite well. ACL strain prediction of the model was validated with a specimen-specific simulation. The validation was achieved without any adjustment to model properties. The properties and assumption used in this model were developed based on previous efforts to build a stand-alone knee model, which includes passive flexion and rotational stiffness tests to ensure proper tibiofemoral behavior (Wilson et al., 2000; Pandy and Shelburne, 1997; Blankevoort et al., 1991; Andriacchi et al., 1983; Crowninshield et al., 1976). After generating this complete simulation model with both the knee and experimental apparatus, we merely compared the results in response to the same impact loading. Thus, the knee model appears to provide reliable results when applying various loading conditions which are difficult to set up in cadaver or in in vivo studies.

In conclusion, the results of this study demonstrate that an external posterior force during landing reduces strain in the ACL, thus reducing ACL injury risk. The use of a specimen-specific computational model gives unique insight into the factors that affect ACL strain and may lead to ACL injuries.

Acknowledgements

The authors acknowledge partial funding from NIH Grant #R01-AR39421. The authors would also like to acknowledge Dr. Withrow, Dr. Ashton-Miller, Dr. Wojtys, and Ms. Huston at the University of Michigan for providing the experimental data, Dr. Thelen at the University of Wisconsin for his advice in building the knee model using ADAMS, and Mr. Koo at Stanford University for providing MRI segmentation software.

References

Abdel-Rahman, E.M., Hefzy, M.S., 1998. Three-dimensional dynamic behaviour of the human knee joint under impact loading. Medical Engineering & Physics 20, 276–290.

Andriacchi, T.P., Mikosz, R.P., Hampton, S.J., Galante, J.O., 1983. Model studies of the stiffness characteristics of the human knee joint. Journal of Biomechanics 16, 23–29.

Andriacchi, T.P., Alexander, E.J., Toney, M.K., Dyrby, C.O., Sum, J., 1998. A point cluster method for in vivo motion analysis: applied to a study of knee kinematics. Journal of Biomechanical Engineering 120, 743–749.

Beynnon, B.D., Howe, J.G., Pope, M.H., Johnson, R.J., Fleming, B.C., 1992. The measurement of anterior cruciate ligament strain in vivo. International Orthopaedics 16, 1–12.

Blackburne, J.S., Peel, T.E., 1977. A new method of measuring patellar height. Journal of Bone and Joint Surgery—British Volume 59, 241–242.

Blankevoort, L., Kuiper, J.H., Huiskes, R., Grootenboer, H.J., 1991. Articular contact in a three-dimensional model of the knee. Journal of Biomechanics 24, 1019–1031.

Boden, B.P., Dean, G.S., Feagin Jr., J.A., Garrett Jr., W.E., 2000. Mechanisms of anterior cruciate ligament injury. Orthopedics 23, 573–578.

Burke, D., Dickson, H.G., Skuse, N.F., 1991. Task-dependent changes in the responses to low-threshold cutaneous afferent volleys in the human lower limb. The Journal of Physiology 432, 445–458.

Caruntu, D.I., Hefzy, M.S., 2004. 3-D anatomically based dynamic modeling of the human knee to include tibio-femoral and patello-femoral joints. Journal of Biomechanical Engineering 126, 44–53.

Chaudhari, A.M., Dyrby, C.O., Andriacchi, T.P., 2004. Anterior tibial translation is not a likely mechanism of anterior cruciate ligament injury during non-contact sports situations. In: International Symposium on Ligaments & Tendons—IV, San Francisco, CA.

Chen, E., Ellis, R.E., Bryant, J.T., Rudan, J.F., 2001. A computational model of postoperative knee kinematics. Medical Image Analysis 5, 317–330.

Clarke, H., Scott, W., Insall, J., Pedersen, H., Math, K., Vigorita, V., Cushner, F., 2001. Antomy. In: Insall, J., Scott, W. (Eds.), Surgery of the Knee. Churchill Livingston, New York, pp. 15–65.

Colby, S., Francisco, A., Yu, B., Kirkendall, D., Finch, M., Garrett Jr., W., 2000. Electromyographic and kinematic analysis of cutting maneuvers. Implications for anterior cruciate ligament injury. The American Journal of Sports Medicine 28, 234–240.

Cooper, D.E., Deng, X.H., Burstein, A.L., Warren, R.F., 1993. The strength of the central third patellar tendon graft. A biomechanical study. The American Journal of Sports Medicine 21, 818–823 discussion 823-4.

Crowninshield, R., Pope, M.H., Johnson, R.J., 1976. An analytical model of the knee. Journal of Biomechanics 9, 397–405.

Fleming, B.C., Beynnon, B.D., Tohyama, H., Johnson, R.J., Nichols, C.E., Renstrom, P., Pope, M.H., 1994. Determination of a zero strain reference for the anteromedial band of the anterior cruciate ligament. Journal of Orthopaedic Research 12, 789–795.

Fleming, B.C., Renstrom, P.A., Beynnon, B.D., Engstrom, B., Peura, G.D., Badger, G.J., Johnson, R.J., 2001. The effect of weightbearing and external loading on anterior cruciate ligament strain. Journal of Biomechanics 34, 163–170.

Fung, D.T., Zhang, L.Q., 2003. Modeling of ACL impingement against the intercondylar notch. Clinical Biomechanics 18, 933–941.

Garg, A., Walker, P.S., 1990. Prediction of total knee motion using a three-dimensional computer-graphics model. Journal of Biomechanics 23, 45–58.

Girgis, F.G., Marshall, J.L., Monajem, A., 1975. The cruciate ligaments of the knee joint. Anatomical, functional and experimental analysis. Clinical Orthopaedics and Related Research 106, 216–231.

Griffin, L.Y., Agel, J., Albohm, M.J., Arendt, E.A., Dick, R.W., Garrett, W.E., Garrick, J.G., Hewett, T.E., Huston, L., Ireland, M.L., Johnson, R.J., Kibler, W.B., Lephart, S., Lewis, J.L., Lindenfeld, T.N., Mandelbaum, B.R., Marchak, P., Teitz, C.C., Wojtys, E.M., 2000. Noncontact anterior cruciate ligament injuries: risk factors and prevention strategies. The Journal of the American Academy of Orthopaedic Surgeons 8, 141–150.

Harner, C.D., Baek, G.H., Vogrin, T.M., Carlin, G.J., Kashiwaguchi, S., Woo, S.L., 1999. Quantitative analysis of human cruciate ligament insertions. Arthroscopy 15, 741–749.

Hewett, T.E., Myer, G.D., Ford, K.R., Heidt Jr., R.S., Colosimo, A.J., McLean, S.G., van den Bogert, A.J., Paterno, M.V., Succop, P., 2005. Biomechanical measures of neuromuscular control and valgus loading of the knee predict anterior cruciate ligament injury risk in female athletes: a prospective study. The American Journal of Sports Medicine 33, 492–501.

Insall, J., Salvati, E., 1971. Patella position in the normal knee joint. Radiology 101, 101–104.

Koo, S., Gold, G.E., Andriacchi, T.P., 2005. Considerations in measuring cartilage thickness using MRI: factors influencing reproducibility and accuracy. Osteoarthritis and Cartilage 13, 782–789.

Lötstedt, P., 1982. Mechanical systems of rigid bodies subject to unilateral constraints. SIAM Journal on Applied Mathematics 42, 281–296.

Markolf, K.L., Burchfield, D.M., Shapiro, M.M., Shepard, M.F., Finerman, G.A., Slauterbeck, J.L., 1995. Combined knee loading states that generate high anterior cruciate ligament forces. Journal of Orthopaedic Research 13, 930–935.

McLean, S.G., Huang, X., Su, A., Van Den Bogert, A.J., 2004. Sagittal plane biomechanics cannot injure the ACL during sidestep cutting 19, 828–838.

Mow, V.C., Ateshian, G.A., Spilker, R.L., 1993. Biomechanics of diarthrodial joints: a review of twenty years of progress. Journal of Biomechanical Engineering 115, 460–467.

Nam, E.K., Makhsous, M., Koh, J., Bowen, M., Nuber, G., Zhang, L.Q., 2004. Biomechanical histological evaluation of osteochondral transplantation in a rabbit model. The American Journal of Sports Medicine 32, 308–316.

Noyes, F.R., Butler, D.L., Grood, E.S., Zernicke, R.F., Hefzy, M.S., 1984. Biomechanical analysis of human ligament grafts used in knee-ligament repairs and reconstructions. Journal of Bone and Joint Surgery—American Volume 66, 344–352.

Olsen, O.E., Myklebust, G., Engebretsen, L., Bahr, R., 2004. Injury mechanisms for anterior cruciate ligament injuries in team handball: a systematic video analysis. The American Journal of Sports Medicine 32, 1002–1012.

Oni, O.O., Morrison, C.J., 1998. The mechanical 'quality' of osteophytes. Injury 29, 31–33.

Pandy, M.G., Shelburne, K.B., 1997. Dependence of cruciate-ligament loading on muscle forces and external load. Journal of Biomechanics 30, 1015–1024.

Reicher, M.A., 1993. An atlas of normal multiplanar anatomy of the knee joint. In: Mink, J.H., Reicher, M.A., Crues, J.V., Deutsch, A.L. (Eds.), Magnetic Resonance Imaging of the Knee. Raven Press, New York, pp. 51–90.

Shelburne, K.B., Pandy, M.G., 1997. A musculoskeletal model of the knee for evaluating ligament forces during isometric contractions. Journal of Biomechanics 30, 163–176.

Shelbourne, K.D., Davis, T.J., Klootwyk, T.E., 1998. The relationship between intercondylar notch width of the femur and the incidence of anterior cruciate ligament tears. A prospective study. The American Journal of Sports Medicine 26, 402–408.

Song, Y., Debski, R.E., Musahl, V., Thomas, M., Woo, S.L., 2004. A three-dimensional finite element model of the human anterior cruciate ligament: a computational analysis with experimental validation. Journal of Biomechanics 37, 383–390.

Wilson, D.R., Feikes, J.D., Zavatsky, A.B., O'Connor, J.J., 2000. The components of passive knee movement are coupled to flexion angle. Journal of Biomechanics 33, 465–473.

Withrow, T.J., Huston, L.J., Wojtys, E.M., Ashton-Miller, J.A., 2006. The relationship between quadriceps muscle force, knee flexion, and anterior cruciate ligament strain in an in vitro simulated jump landing. The American Journal of Sports Medicine 34, 269–274.

Woo, S.L., Hollis, J.M., Adams, D.J., Lyon, R.M., Takai, S., 1991. Tensile properties of the human femur-anterior cruciate ligament-tibia complex. The effects of specimen age and orientation. The American Journal of Sports Medicine 19, 217–225.

Woo, S.L., Debski, R.E., Withrow, J.D., Janaushek, M.A., 1999. Biomechanics of knee ligaments. The American Journal of Sports Medicine 27, 533–543.

Woo, S.L., Kanamori, A., Zeminski, J., Yagi, M., Papageorgiou, C., Fu, F.H., 2002. The effectiveness of reconstruction of the anterior cruciate ligament with hamstrings and patellar tendon. A cadaveric study comparing anterior tibial and rotational loads. Journal of Bone and Joint Surgery—American Volume 84-A, 907–914.

Woo, S.L., Abramowitch, S.D., Kilger, R., Liang, R., 2006. Biomechanics of knee ligaments: injury, healing, and repair. Journal of Biomechanics 39, 1–20.

Yu, C.H., Walker, P.S., Dewar, M.E., 2001. The effect of design variables of condylar total knees on the joint forces in step climbing based on a computer model. Journal of Biomechanics 34, 1011–1021.